Inorganic Chemistry

Article

pubs.acs.org/IC

Acid-Induced Degradation of Phosphorescent Dopants for OLEDs and Its Application to the Synthesis of Tris-heteroleptic Iridium(III) Bis-cyclometalated Complexes

Etienne Baranoff,*[,†] Basile F. E. Curchod,[‡] Julien Frey,[†] Rosario Scopelliti,[†] Florian Kessler,[†] Ivano Tavernelli,[‡] Ursula Rothlisberger,[‡] Michael Grätzel,[†] and Md. Khaja Nazeeruddin[†]

[†]Laboratory of Photonics and Interfaces and [‡]Laboratory of Computational Chemistry and Biochemistry, Institute of Chemical Sciences and Engineering, School of Basic Sciences, École Polytechnique Fédérale de Lausanne, CH-1015 Lausanne, Switzerland

Supporting Information

ABSTRACT: Investigations of blue phosphorescent organic light emitting diodes (OLEDs) based on [Ir(2-(2,4-difluorophenyl)-pyridine)$_2$(picolinate)] (FIrPic) have pointed to the cleavage of the picolinate as a possible reason for device instability. We reproduced the loss of picolinate and acetylacetonate ancillary ligands in solution by the addition of Brønsted or Lewis acids. When hydrochloric acid is added to a solution of a [Ir(C^N)$_2$(X^O)] complex (C^N = 2-phenylpyridine (ppy) or 2-(2,4-difluorophenyl)pyridine (diFppy) and X^O = picolinate (pic) or acetylacetonate (acac)), the cleavage of the ancillary ligand results in the direct formation of the chloro-bridged iridium(III) dimer [{Ir(C^N)$_2$(μ-Cl)}$_2$]. When triflic acid or boron trifluoride are used, a source of chloride (here tetrabutylammonium chloride) is added to obtain the same chloro-bridged iridium(III) dimer. Then, we advantageously used this degradation reaction for the efficient synthesis of tris-heteroleptic cyclometalated iridium(III) complexes [Ir(C^N^1)(C^N^2)(L)], a family of cyclometalated complexes otherwise challenging to prepare. We used an iridium(I) complex, [{Ir(COD)(μ-Cl)}$_2$], and a stoichiometric amount of two different C^N ligands (C^N^1 = ppy; C^N^2 = diFppy) as starting materials for the swift preparation of the chloro-bridged iridium(III) dimers. After reacting the mixture with acetylacetonate and subsequent purification, the tris-heteroleptic complex [Ir(ppy)(diFppy)(acac)] could be isolated with good yield from the crude containing as well the bis-heteroleptic complexes [Ir(ppy)$_2$(acac)] and [Ir(diFppy)$_2$(acac)]. Reaction of the tris-heteroleptic acac complex with hydrochloric acid gives pure heteroleptic chloro-bridged iridium dimer [{Ir(ppy)(diFppy)(μ-Cl)}$_2$], which can be used as starting material for the preparation of a new tris-heteroleptic iridium(III) complex based on these two C^N ligands. Finally, we use DFT/LR-TDDFT to rationalize the impact of the two different C^N ligands on the observed photophysical and electrochemical properties.

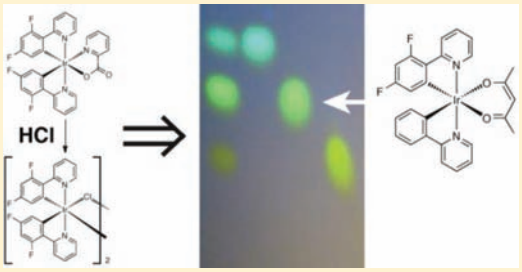

INTRODUCTION

The efficiency of organic light-emitting devices (OLEDs) can be significantly improved with phosphorescent emitters that harvest both the singlet and triplet excitons formed by the recombination of free charge carriers.[1] However, the short lifetime of phosphorescent blue OLEDs is an important issue that impedes the development of this promising technology. Many reasons for the loss of luminescence are general to all OLEDs,[2,3] and solutions to extrinsic problems have significantly progressed with improved fabrication and encapsulation processes. Therefore, recent research aims at understanding the chemical degradation of the organic materials used in the devices, that creates *in situ* new chemical species acting as nonradiative recombination centers.[4]

FIrPic[5] ([Ir(2-(2,4-difluorophenyl)pyridine)$_2$(picolinate)] or simply [Ir(diFppy)$_2$(pic)]) has received special attention as a sky blue phosphorescent emitter. High-performance liquid chromatography coupled to mass spectrometry (HPLC-MS)[6] and laser-desorption/ionization time-of-flight mass spectrometry (LDI-TOF-MS)[7] have been used to analyze the chemical degradation in stressed devices based on FIrPic. Accordingly, the loss of efficiency has been attributed in part to isomerization of FIrPic from the *N,N*-trans isomer (the two pyridine rings of the diFppy main ligands are trans to each other) to the *N,N*-cis isomer (the two pyridine rings of the diFppy main ligands are cis to each other), which follows our report regarding the thermal isomerization of FIrPic.[8] In addition, using an heteroleptic emitter exhibiting more propensity to isomerization, we have shown that the presence of the *N,N*-cis isomer as an impurity along the *N,N*-trans isomer reduces significantly the efficiency of the device.[9] A second reason for the instability of the device has been attributed to the dissociation of the picolinate ancillary ligand and the concomitant formation of the [Ir(diFppy)$_2$]$^+$ fragment. The latter could act as trap states for excitons and charges either as such or after reaction with surrounding molecules, as it has been recently found in a device based on the tris-

Received: July 12, 2011
Published: December 9, 2011

 © 2011 American Chemical Society dx.doi.org/10.1021/ic202162q | *Inorg. Chem.* 2012, 51, 215−224

homoleptic complex tris(2-phenylpyridine)iridium(III) (Ir(ppy)$_3$).[10] By analogy with ruthenium-based molecular machines,[11] the general mechanism for ligand cleavage is tentatively attributed to the thermal accessibility of the metal-centered (MC) states.[12,13]

As a further step to link the chemistry of the materials to the stability of the devices, in the first part of the manuscript, we report the acid-induced cleavage of the picolinate and acetylacetonate ancillary ligands in bis-cyclometalated iridium complexes. Since protons are likely to be present in the emissive layer upon aging of hole transporting materials[14] or through the use of PEDOT:PSS,[15] this acid-induced degradation mechanism could reasonably explain why the devices based on emitters having N^O or O^O ancillary ligands are significantly less stable than their tris-cyclometalated counterparts.

While being a significant drawback for the stability of OLEDs, we used then the chemistry behind the acid-induced degradation to our advantage for the preparation of tris-heteroleptic complexes [Ir(C^N^1)(C^N^2)(L)]. The synthesis of this class of compounds is a real synthetic challenge, resulting in only little information in the literature about their properties despite their potential interest for the preparation of multifunctional phosphorescent molecules. Indeed, each ligand could be used for implementing a specific function such as sensing, anchoring, and solubilizing. As far as we know, such complexes have been reported only as part of a mixture[16] or with very low yield, around 10%.[17,18] We report now a strategy for the efficient synthesis of tris-heteroleptic complexes. It is based first on the use of the iridium(I) complex [{Ir(COD)(μ-Cl)}$_2$] for the swift and efficient synthesis of cyclometalated chloro-bridged iridium(III) dimers and second on the acid-induced degradation reaction to recover the pure heteroleptic dimer [{Ir(C^N^1)(C^N^2)(μ-Cl)}$_2$] from the purified acetylacetonate tris-heteroleptic complex [Ir(C^N^1)(C^N^2)(acac)]. The pure heteroleptic dimer can be subsequently used for the preparation of tris-heteroleptic complexes without anymore the burden of tedious purification of mixtures of complexes. Finally, with the help of theoretical calculation, we discuss the impact of having two different cyclometalated ligands on the shape of the emission spectrum.

EXPERIMENTAL PROCEDURES

Materials and General Considerations. All materials and solvents were of reagent quality and used as received. [{Ir(COD)Cl}$_2$] was purchased from Strem, 2-phenylpyridine from Aldrich, and acetylacetone from Fluka. ^{1}H and ^{13}C NMR spectra were recorded using a Bruker AV 400 MHz spectrometer. Chemical shifts δ (in ppm) are referenced to residual solvent peaks. ^{19}F NMR spectra were recorded using a Bruker AV 200 MHz spectrometer. Coupling constants are expressed in hertz (Hz). High-resolution mass spectra (HRMS) and elemental analysis have been performed with the Service d'Analyze of EPFL. UV−visible spectra were recorded in a 1 cm path length quartz cell on a Hewlett Packard 8453 spectrophotometer. Emission spectra were recorded on a Fluorolog 3-22 using a 90° optical geometry. The quantum yields were determined using quinine sulfate (10^{-5} M in 1 M H_2SO_4; air equilibrated; QY = 0.546) and [Ru(bpy)$_3$][PF$_6$]$_2$ (10^{-5} M in water; air equilibrated; QY = 0.028) as standards. Excited-state lifetimes were measured using a FL-1061PC TCSPC and 406 nm Nanoled as excitation source. Solutions were degassed by bubbling argon softly for 30 min. Voltammetric measurements employed a PC controlled AutoLab PSTAT10 electrochemical workstation and were carried out in an Ar-filled glovebox, with oxygen and water < 5 ppm. All experiments were realized using 0.1 M TBAPF$_6$ in anhydrous DMF as electrolyte using a carbon glassy electrode and two Pt wires as working, counter, and reference electrodes, respectively. Ferrocene was used as internal standard. A scan rate of 100 mV·s^{-1} has been applied. Before each measurement, samples were stirred for 15 s and left to equilibrate for 5 s.

X-ray Crystal Structure Determination. The data collection for the crystal structure was measured at low temperature [100(2) K] using Mo Kα radiation on a Bruker APEX II CCD equipped with a κ geometry goniometer. The data were reduced by EvalCCD[19] and then corrected for absorption.[20] The solution and refinement were performed with SHELX.[21] The structure was refined using full-matrix least-squares based on F^2 with all non-hydrogen atoms anisotropically defined. Hydrogen atoms were placed in calculated positions by means of the "riding" model. Disorder problems dealing with the fluorine atoms and corresponding hydrogens were found during the last stages of refinement and solved using the split model.

Computational Details. Full geometry optimizations of the iridium compounds (**2** and [Ir(diFppy)$_2$(acac)]) in their singlet ground state were performed with DFT with ultrafine grid and tight convergence criteria using the M06 functional,[22] with the relativistic effective core potential and basis set LANL2DZ[23] for the iridium and the 6-311G*[24] basis set for the remaining atoms. No symmetry constraints were applied during the geometry optimizations, which were carried out with the Gaussian 09 package.[25] The nature of the stationary points located was further checked by computations of harmonic vibrational frequencies at the same level of theory. At each ground state (singlet) geometry, LR-TDDFT calculations were performed using the same basis sets and *xc*-functional. Condensed-phase effects were taken into account for geometry optimization and spectra calculations using a self-consistent reaction-field (SCRF) model in which the solvent is implicitly represented by a dielectric continuum characterized by its relative static dielectric permittivity ε. The solute, which is placed in a cavity created in the continuum after spending some cavitation energy, polarizes the continuum, which in turn creates an electric field inside the cavity. Within the different approaches that can be followed to calculate the electrostatic potential created by the polarized continuum in the cavity, we have employed the integral equation formalism of the polarizable continuum model (IEFPCM).[26] As the solvent molecules have no time to geometrically rearrange within the time of a vertical excitation, nonequilibrium solvation[27] has been used for the LR-TDDFT calculations of absorption spectra. A relative permittivity of 8.93 was employed to simulate dichloromethane,[25] the solvent used in the experimental work.

To gain insights into the phosphorescence behavior of the different iridium compounds, we optimized the geometry of the first two triplet states using unrestricted DFT (U-DFT) with the same basis set as described before. As suggested by a recent work,[28] we used the *xc*-functional M05-2X[29] for this task, due to its excellent performance for the emission spectra for a series of iridium-based compounds. At the minimum energy structure, we computed the difference in energy between the triplet state (T_{1a} or T_{1b}) and singlet state (S_0) with the inclusion of implicit solvent and obtained an estimation of the first phosphorescence band. Additional LR-TDDFT calculations at T_{1a} and T_{1b} geometry were done using the same conditions as those described above. It is worth noting that the same trends between excited states are observed using M06 and M05-2X. On the basis of the DFT triplet geometries, spin−orbit coupling (SOC) LR-TDDFT/M06 calculations were performed with the ADF2009 package[30,31] using the ZORA methodology.[32] All electron basis sets have been used for all the atoms (iridium, TZP; all other atoms, DZP), and solvent effects have been described with the conductor-like screening (COSMO) model.[33,34]

General Method for the Synthesis of Chloro-bridged Dimer Complexes. A [{Ir(COD)Cl}$_2$] dimer (2.00 g, 2.98 mmol) was suspended in 9 mL of 2-ethoxyethanol in a 50 mL flask. The suspension was filled with argon by 3 cycles vacuum/argon. The ligand L (11.95 mmol, 4 equiv) was added, and 1 mL of 2-ethoxyethanol was used for rinsing. The mixture was filled again with argon by 3 cycles vacuum/argon. The flask was sealed and heated at 130 °C for 3 h. Upon heating, the solution darkens to a deep red-orange color. Within

dx.doi.org/10.1021/ic202162q | Inorg. Chem. 2012, 51, 215−224

half an hour, a yellow precipitate appears. After 3 h, the volume of solvent was reduced under vacuum and 20 mL of methanol was added and the precipitate filtered, washed with methanol, and dried to afford the chloro-bridged iridium dimer $[\{Ir(L)_2(\mu\text{-}Cl)\}_2]$.

General Method for the Synthesis of Acetylacetonate Complexes. Acetylacetone (4 equiv) and tetrabutylammonium hydroxide (3 equiv) were mixed in dichloromethane/methanol, 10/1 volume to volume, and this solution was added to a solution of the corresponding dimer in dichloromethane. The solution was gently refluxed (about 40 °C) under argon overnight. After cooling down to room temperature, the solution was evaporated to dryness to give a yellow viscous oil which precipitates upon addition of methanol and deionized water. The suspension was kept in the fridge for 2 h, filtered off, and washed with water. The solid was adsorbed on silica, deposited on the top of a silica gel chromatography column, and eluted with dichloromethane. Finally, the main fraction was dissolved in a minimum amount of dichloromethane and slowly precipitated with hexane. The suspension was filtered off, washed with hexane, and dried to afford $[Ir(L)_2(acac)]$ complexes as solids.

$[\{Ir(ppy)_2(\mu\text{-}Cl)\}_2]$. L was 2-phenylpyridine (ppy). The chloro-bridged iridium dimer $[\{Ir(ppy)_2(\mu\text{-}Cl)\}_2]$ was obtained as an orange solid (2.94 g, 2.74 mmol, yield = 92%). ^{1}H NMR ($CDCl_3$, 400 MHz): δ 9.26 (dd, 4H, J = 6.0, 0.8 Hz); 7.88 (d, 4H, J = 8.0 Hz); 7.56 (dt, 4H, J = 8.0, 1.6 Hz); 7.51 (dd, 4H, J = 8.0, 1.2 Hz); 6.79 (dt, 4H, J = 6.0, 1.2 Hz); 6.76 (dt, 4H, J = 8.4, 1.2 Hz); 6.58 (dt, 4H, J = 8.0, 1.2 Hz); 5.95 (dd, 4H, J = 7.6, 1.2 Hz). ^{1}H NMR ($CDCl_3$ + DMSO, 400 MHz): δ 9.86 (d, 1H, J = 5.6 Hz); 9.72 (d, 1H, J = 6.0 Hz); 7.87−81 (m, 3H); 7.76 (dt, 1H, J = 8.4, 1.2 Hz); 7.49 (dd, 2H, J = 7.6, 1.2 Hz); 7.29 (dt, 1H, J = 7.2, 3.2 Hz); 7.21 (dt, 1H, J = 6.0, 1.6 Hz); 6.86 (dt, 1H, J = 7.2, 0.8 Hz); 6.81 (dt, 1H, J = 8.0, 0.8 Hz); 6.74 (dt, 1H, J = 7.6, 1.2 Hz); 6.68 (dt, 1H, J = 7.6, 1.2 Hz); 6.40 (d, 1H, J = 7.2 Hz); 5.73 (d, 1H, J = 6.8 Hz).

$[Ir(ppy)_2(acac)]$. Using $[\{Ir(ppy)_2(\mu\text{-}Cl)\}_2]$ (950 mg, 0.88 mmol). $[Ir(ppy)_2(acac)]$ was obtained as an orange solid (946 mg, yield 89%). ^{1}H NMR ($CDCl_3$, 400 MHz): δ 8.51 (ddd, 2H, J = 6.0, 1.6, 0.8 Hz); 7.84 (dd, 2H, J = 7.2, 0.8 Hz); 7.72 (ddd, 2H, J = 8.4, 7.6, 1.6 Hz); 7.54 (dd, 2H, J = 8.0, 1.2 Hz); 7.13 (ddd, 2H, J = 7.6, 6.0, 1.6 Hz); 6.80 (dt, 2H, J = 7.6, 1.2 Hz); 6.68 (dt, 2H, J = 7.6, 1.6 Hz); 6.26 (dt, 2H, J = 8.0, 1.2 Hz); 5.21 (1H, s); 1.78 (6H, s). ESI-TOF HRMS MH^+ m/z: calc 600.1390, found 600.1339.

$[\{Ir(diFppy)_2(\mu\text{-}Cl)\}_2]$. L was 2-(2,4-difluorophenyl)pyridine (diFppy). The chloro-bridged iridium dimer $[\{Ir(diFppy)_2(\mu\text{-}Cl)\}_2]$ was obtained as a yellow solid (3.40 g, 2.70 mmol, yield = 90%). ^{1}H NMR ($CDCl_3$, 400 MHz): δ 9.11 (ddd, 4H, J = 6.4, 1.6, 0.8 Hz); 8.30 (ddd, 4H, J = 9.2, 0.8, 0.4 Hz); 7.83 (dt, 4H, J = 8.4, 1.2 Hz); 6.83 (ddd, 4H, J = 7.6, 6.0, 1.2 Hz); 6.34 (ddd, 4H, J = 12.4, 8.8, 2.0 Hz); 5.28 (dd, 4H, J = 9.2, 2.0 Hz). ^{1}H NMR ($CDCl_3$ + DMSO, 400 MHz): δ 9.86 (d, 1H, J = 5.6 Hz); 9.78 (d, 1H, J = 5.2 Hz); 8.33 (d, 1H, J = 7.2 Hz); 8.29 (d, 1H, J = 9.4 Hz); 7.97 (t, 1H, J = 7.6 Hz); 7.87 (t, 1H, J = 8.0 Hz); 7.39 (t, 1H, J = 6.0 Hz); 7.32 (t, 1H, J = 6.0 Hz); 6.47 (ddd, 1H, J = 12.0, 9.2, 2.4 Hz); 6.39 (ddd, 1H, J = 12.0, 9.2, 2.4 Hz); 5.91 (dd, 1H, J = 8.0, 2.0 Hz); 5.19 (dd, 1H, J = 8.8, 2.0 Hz).

$[Ir(diFppy)_2(acac)]$. Using $[\{Ir(diFppy)_2(\mu\text{-}Cl)\}_2]$ (950 mg, 0.78 mmol), $[Ir(diFppy)_2(acac)]$ was obtained as a bright yellow solid (976 mg, yield 93%). ^{1}H NMR ($CDCl_3$, 400 MHz): δ 8.43 (ddd, 2H, J = 6.0, 2.0, 0.8 Hz); 8.24 (d, 2H, J = 8.4 Hz); 7.79 (tdd, 2H, J = 7.2, 1.6, 0.8 Hz); 7.18 (ddd, 2H, J = 7.6, 5.6, 1.2 Hz); 6.32 (ddd, 2H, J = 12.8, 9.6, 2.4 Hz); 5.64 (dd, 2H, J = 8.8, 2.4 Hz); 5.24 (s, 1H); 1.80 (s, 6H). ^{19}F NMR ($CDCl_3$, 188 MHz): δ −108.79 (quadruplet, J = 9.9 Hz); −111.05 (triplet, J = 12.1 Hz). ESI-TOF HRMS MH^+ m/z: calc 672.1013, found 672.1060.

Mixture Containing the Heteroleptic Dimer 1, $[\{Ir(ppy)(diFppy)(\mu\text{-}Cl)\}_2]$. L was an equimolar mixture of diFppy (2 equiv) and ppy (2 equiv). 1.055 g (1.57 mmol) of $[\{Ir(COD)Cl\}_2]$ was used. The mixture of chloro-bridged iridium dimers, $[Ir_2(ppy)_{4-n}(diFppy)_n(\mu\text{-}Cl)_2]$, n = 0−4, was obtained as a yellow solid (1.57 g, 1.50 mmol, yield = 96%, assuming only **1** was obtained).

$[Ir(ppy)(diFppy)(acac)]$ 2. Using the mixture of dimers containing **1** (1.503 g, 1.44 mmol). **2** was obtained as a bright yellow solid (808 mg, 1.27 mmol, yield 44%). ^{1}H NMR ($CDCl_3$, 400 MHz): δ 8.50 (ddd, 1H, J = 6.0, 1.6, 0.8 Hz); 8.44 (ddd, 1H, J = 5.2, 1.6, 0.8 Hz); 8.22 (d, 1H, J = 8.4 Hz); 7.86 (d, 1H, J = 8.4 Hz); 7.75 (m, 2H); 7.56 (dd, 1H, J = 7.6, 1.2 Hz); 7.16 (m, 2H); 6.85 (dt, 1H, J = 7.6, 1.2 Hz); 6.74 (dt, 1H, J = 7.6, 1.2 Hz); 6.26 (ddd, 1H, J = 12.8, 9.6, 2.4 Hz); 6.20 (dd, 1H, J = 7.6, 0.8 Hz); 5.70 (dd, 1H, J = 8.8, 2.4 Hz); 5.23 (s, 1H); 1.82 (s, 3H); 1.78 (s, 3H). ^{19}F NMR ($CDCl_3$, 188 MHz): δ −109.38 (quadruplet, J = 10.1 Hz); −111.66 (triplet, J = 12.0 Hz). ESI-TOF HRMS: MH^+ m/z: calc 636.1202, found 636.1225. Anal. Calcd for $C_{27}H_{21}F_2IrN_2O_2$: C, 51.01; H, 3.33; N, 4.41. Found: C, 50.84; H, 3.37; N, 4.38.

Pure 1 $[\{Ir(ppy)(diFppy)(\mu\text{-}Cl)\}_2]$. HCl in a solution in diethyl ether (2 N, 1 mL) was added to a solution of **2** (407 mg, 0.64 mmol) in dichloromethane (80 mL), and the solution was stirred for 15 min at room temperature. Methanol was added, and the dichloromethane and ether were evaporated. The suspension was filtered, washed with methanol, and dried. Pure **1** (as a mixture of two isomers) was obtained as a yellow solid (287 mg, 0.27 mmol, yield 86%). ^{1}H NMR ($CDCl_3$, 400 MHz): δ 9.20 (dt, 4H, J = 5.6, 0.8 Hz); 9.13 (dt, 4H, J = 5.8, 0.8 Hz); 8.25 (d, 4H, J = 7.6 Hz); 7.88 (d, 4H, J = 8.2 Hz); 7.78−7.73 (m, 8H); 7.50 (ddd, 4H, J = 7.8, 3.2, 1.0 Hz); 6.82−6.74 (m, 12H); 6.59 (m, 4H); 6.26 (m, 4H); 5.82 (d, 4H, J = 7.8 Hz); 5.35 (dd, 4H, J = 9.2, 1.2 Hz). ^{19}F NMR ($CDCl_3$, 188 MHz): δ −108.58 (quintuplet, J = 10.3 Hz); −111.08 (quadruplet, J = 10.7 Hz). Anal. Calcd for $C_{44}H_{28}Cl_2F_4Ir_2N_4$: C, 46.19; H, 2.47; N, 4.90. Found: C, 45.83; H, 2.40; N, 4.77. ^{1}H NMR ($CDCl_3$ + 2 drops of DMSO-d_6, 400 MHz): δ 9.70 (d, 0.6H, J = 5.6 Hz); 9.57 (d, 0.4H, J = 5.6 Hz); 9.52 (d, 0.4H, J = 5.8 Hz); 9.44 (d, 0.6H, J = 5.8 Hz); 8.03 (d, 0.4H, J = 8.6 Hz); 8.00 (d, 0.6H, J = 8.6 Hz); 7.79−7.60 (m, 3H); 7.37−7.31 (m, 1H); 7.16−7.11 (m, 1H); 7.09−7.03 (m, 1H); 6.71 (t, 0.6H, J = 7.6 Hz); 6.65 (t, 0.4H, J = 7.6 Hz); 6.58 (t, 0.6H, J = 7.4 Hz); 6.51 (t, 0.4H, J = 7.4 Hz); 6.20−6.04 (m, 1.6H); 5.63 (dd, 0.4H, J = 8.7, 2.2 Hz); 5.46 (d, 0.4H, J = 7.7 Hz); 4.98 (dd, 0.6H, J = 8.8, 2.2 Hz). ^{19}F NMR ($CDCl_3$ + 2 drops DMSO-d_6, 188 MHz): δ −100.99 (≈40%, quadruplet, J = 9.7 Hz); −103.05 (≈60%, quadruplet, J = 9.8 Hz); −104.44 (≈40%, triplet, J = 11.9 Hz); −105.53 (≈60%, triplet, J = 11.5 Hz).

$[Ir(ppy)(diFppy)(acac)]$ 2 from Pure 1. Sodium acetylacetonate (4 equiv) was added to a solution of pure **1** (98 mg) in a mixture of dichloromethane/methanol (20 mL/5 mL), and the mixture was refluxed overnight. After cooling down to room temperature, the solution was evaporated to dryness and dichloromethane was added and the suspension filtered to remove unreacted sodium acetylacetonate and NaCl. Evaporation of the yellow solution affords a crude solid whose ^{1}H NMR spectrum indicates it to be **2** with very good purity with quantitative yield. See Figure S15 of the Supporting Information for the ^{1}H NMR spectrum of **2** isolated from a reaction of a mixture of dimers and Figure S17 for that of crude **2** from a reaction with pure **1**.

RESULTS AND DISCUSSION

Acid-Induced Degradation. A series of observations motivated us to examine the effect of acids on heteroleptic iridium(III) complexes with N^O or O^O ancillary ligands. First, mass spectrometry of $[Ir(C^N)_2(X^O)]$ neutral complexes, X^O = N^O or O^O ligand, usually gives a signal for the fragment $[Ir(C^N)_2]^+$ in addition to the protonated complex $[Ir(C^N)_2(X^O)(H)]^+$.[35] Second, the synthesis of fac-tris homoleptic complexes $[Ir(C^N)_3]$ from $[Ir(acac)_3]$ uses a HCl-based workup to isolate the final complexes.[36] Then, acids are known to facilitate the isomerization of tris-cyclometalated complexes from mer to fac.[37] Finally, we observed on several occasions a significant amount of the chloro-bridged iridium dimer after purification of complexes with N^O or O^O ancillary ligand by column chromatography eluted with chlorinated solvents whereas the crude of the reaction showed no signals corresponding to the chloro-bridged dimer when checked by ^{1}H NMR.

dx.doi.org/10.1021/ic202162q | Inorg. Chem. 2012, 51, 215−224

We monitored the effect of acids on heteroleptic iridium(III) complexes with N^O or O^O ancillary ligands by ^{1}H NMR (Scheme 1). When hydrochloric acid in solution in diethyl ether is added to a FIrPic solution in $CDCl_3$, the signals for FIrPic disappear and six new peaks corresponding to the chloro-bridged iridium dimer $[\{Ir(diFppy)_2(\mu\text{-}Cl)\}_2]$ appear (Figure 1). Picolinic acid precipitates out of the solution and, therefore, is not observed anymore in the ^{1}H NMR spectrum.

Scheme 1. Acid-Induced Degradation of Complexes in Solution[a]

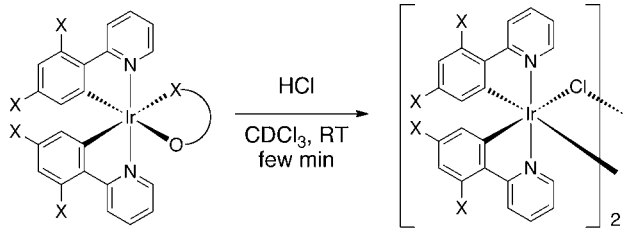

X = -F; X^O = pic : **FIrpic**
X = -F; X^O = acac : **[Ir(diFppy)$_2$(acac)]**
X = -H; X^O = acac : **[Ir(ppy)$_2$(acac)]**

X = -F : **[{Ir(diFppy)$_2$(μ-Cl)}$_2$]**
X = -H : **[{Ir(ppy)$_2$(μ-Cl)}$_2$]**

[a]A few minutes corresponds to the time needed to measure the ^{1}H NMR spectrum.

In the case of $[Ir(ppy)_2(acac)]$ (Figure 2) and $[Ir(diFppy)_2(acac)]$ (full spectra in Figure S1), the starting acac complexes similarly decompose to the chloro-bridged iridium(III) dimers. The coordinated acac is a good probe whose signals (at 5.21 and 1.78 ppm, and 5.26 and 1.82 ppm, for ppy- and diFppy-based complexes, respectively) convert upon acidification to free acetylacetone that is clearly seen as its keto−enol form (four singlets at 5.51, 3.60, 2.25, and 2.06 ppm).

To extend the scope of this acid-induced degradation reaction, we explored acidic systems other than hydrochloric acid. To obtain the final chloro-bridged dimer, we added a source of chloride, namely tetrabutylammonium chloride (TBACl), in the $CDCl_3$ solution of the complex. As expected, the iridium complex is stable in the presence of TBACl (Figure 3a). However, upon addition of a dilute solution of triflic acid (Figure 3b) or boron trifluoride BF_3 (Figure 3c), new peaks corresponding to the chloro-bridged iridium dimer are observed. In every case, the acid-induced cleavage of the ancillary ligand is very efficient and very clean; upon addition of an excess of acid, complete conversion is achieved within a few minutes, which is the time needed to start the measurements of ^{1}H NMR spectra.

Finally, we tested PEDOT:PSS as a source of protons. PEDOT:PSS is a commonly used material in solution processed OLEDs[38] and is a highly acidic material due to the presence of PSS groups. To a NMR tube containing a $CDCl_3$ solution of $[Ir(ppy)_2(acac)]$ and TBACl were added two drops of an aqueous solution of PEDOT:PSS. Because of the heterogeneity of the water/$CDCl_3$ system, the cleavage of the ancillary ligand is much slower (Figure S2 of the Supporting Information). After 2 h, the chloro-bridged dimer is only observed in small quantities, and after 4 weeks, the reaction is close to completion.

Our results show that acids, both Brønsted and Lewis, can be efficient promotters of the cleavage of the N^O and O^O ancillary ligands in heteroleptic iridium(III) complexes. The degradation is particularly efficient in solution. In OLEDs, protons are also likely to be present in the emissive layer upon chemical degradation of hole transporting materials[14] or through the use of PEDOT:PSS.[15] In addition to the thermally accessible MC states, these protons could be one reason for the observed[6,7] degradation of the heteroleptic phosphorescent emitters in aged devices. In particular, they could explain the significantly lower stability of bis-heteroleptic phosphorescent emitters compared to the tris-homoleptic complexes, as bis-heteroleptic iridium(III) complexes are often designed with N^O or O^O ancillary ligands.

Synthesis of Tris-heteroleptic Complexes. Standard synthesis of bis-heteroleptic cyclometalated iridium(III) complexes is usually achieved through a two-step procedure.[39] First, the chloro-bridged iridium(III) dimer is prepared by refluxing

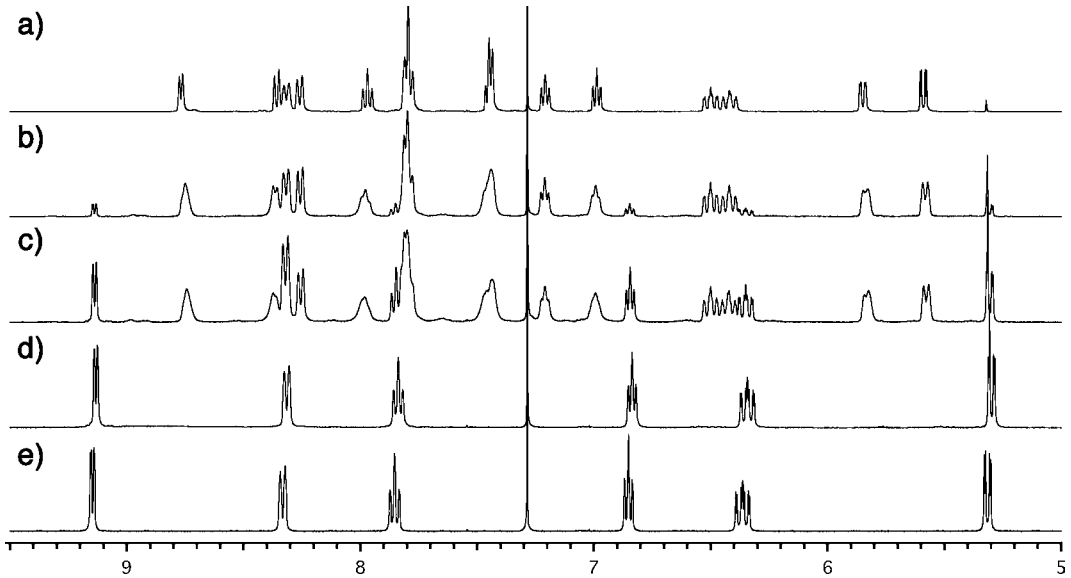

Figure 1. Aromatic part of the ^{1}H NMR in $CDCl_3$: (a) FIrPic; (b, c, d) gradual addition of HCl (ca. 0.2 M in $Et_2O/CDCl_3$); (e) $[\{Ir(diFppy)_2(\mu\text{-}Cl)\}_2]$.

dx.doi.org/10.1021/ic202162q | Inorg. Chem. 2012, 51, 215−224

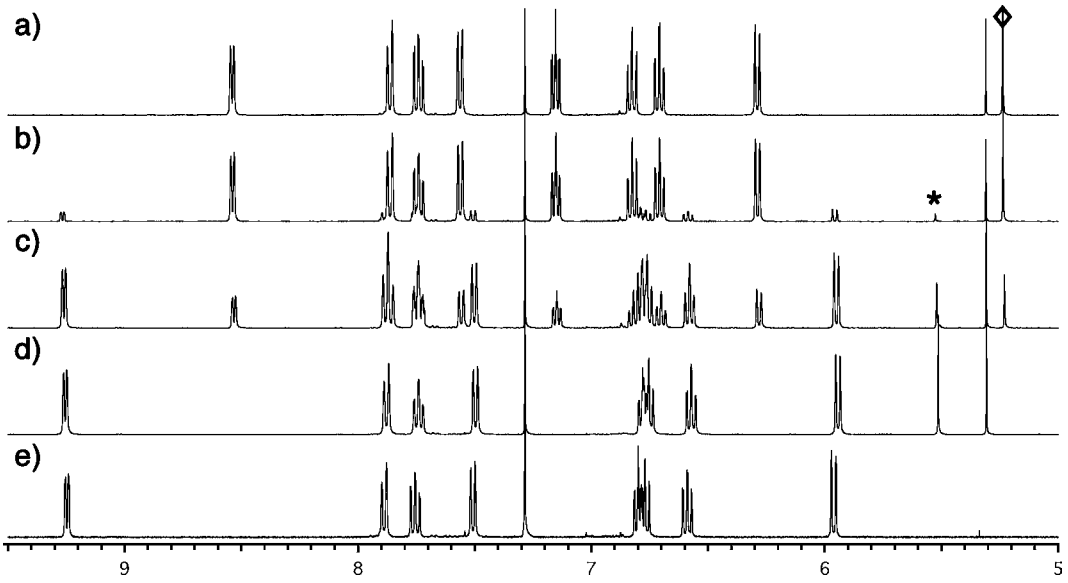

Figure 2. Aromatic part of the ^{1}H NMR in $CDCl_3$: (a) $[Ir(ppy)_2(acac)]$; (b, c, d) gradual addition of HCl (*ca.* 0.2 M in $Et_2O/CDCl_3$); (e) $[\{Ir(ppy)_2(\mu\text{-}Cl)\}_2]$. ◇, signals for the coordinated acac; ∗, signals for free acetylacetone (keto−enol).

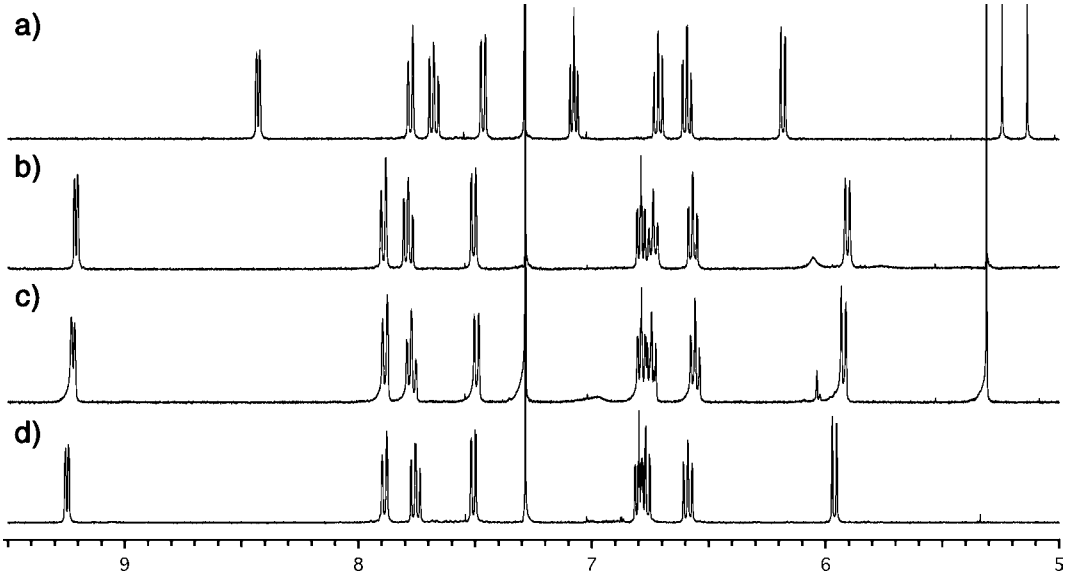

Figure 3. Aromatic part of the ^{1}H NMR in $CDCl_3$: (a) $[Ir(ppy)_2(acac)]$ containing TBACl; (b) addition of triflic acid (10% in $CDCl_3$) to the $[Ir(ppy)_2(acac)]$ solution containing TBACl; (c) addition of BF_3 (1 M in Et_2O) to the $[Ir(ppy)_2(acac)]$ solution containing TBACl; (d) $[\{Ir(ppy)_2(\mu\text{-}Cl)\}_2]$.

the desired ligand with $IrCl_3$, usually as a hydrate, in a mixture of water and 2-ethoxyethanol for 12 to 24 h. Second, the chlorides are replaced with the desired ancillary ligand by refluxing the dimer with this ligand in the presence of a base if necessary. In our hands, this synthetic approach was not successful for the preparation of tris-heteroleptic complexes. Only low yields comparable to those reported in the literature were obtained, and the reproducibility was poor. Moreover, time-consuming and often tedious purifications were necessary for each new tris-heteroleptic complex. Therefore, we looked for a quicker and more efficient approach which revolves around an iridium(I) complex as starting material (Scheme 2). Iridium(I) complexes are common in catalysis but used marginally as starting materials for phosphorescent emitters.[40,41] We found only one recent example using phenylpyridine as cyclometalated ligand with $[\{Ir(COE)_2(\mu\text{-}Cl)\}_2]$ (COE = *cis*-cyclooctene) complex as starting material.[42] We preferred the use of $[\{Ir(COD)(\mu\text{-}Cl)\}_2]$ (COD = 1,5-cyclooctadiene), which, in our hands, appears easier to prepare. With phenylpyridine type ligands, we could prepare the corresponding homoleptic chloro-bridged iridium dimers almost quantitatively within 3 h, which is a significant improvement over the classical procedure.

When two different C^N ligands are used, in this case 2-phenylpyridine (ppy) and 2-(2,4-difluorophenyl)pyridine (diFppy), it results in a mixture of chloro-bridged dimers $[Ir_2(ppy)_{4-n}(diFppy)_n(\mu\text{-}Cl)_2]$ with n = 0−4 that contains dimer **1**, $[\{Ir(ppy)(diFppy)(\mu\text{-}Cl)\}_2]$. This mixture is directly reacted with acetylacetonate (acac) and tetrabutylammonium hydroxide (TBAOH), leading to a statistical mixture of the mononuclear complexes $[Ir(ppy)_2(acac)]$ and $[Ir(diFppy)_2(acac)]$ and complex **2**, $[Ir(ppy)(diFppy)(acac)]$

dx.doi.org/10.1021/ic202162q | *Inorg. Chem.* 2012, 51, 215−224

Scheme 2. Synthetic Strategy for Pure Heteroleptic Dimer 1 and Complex 2[a]

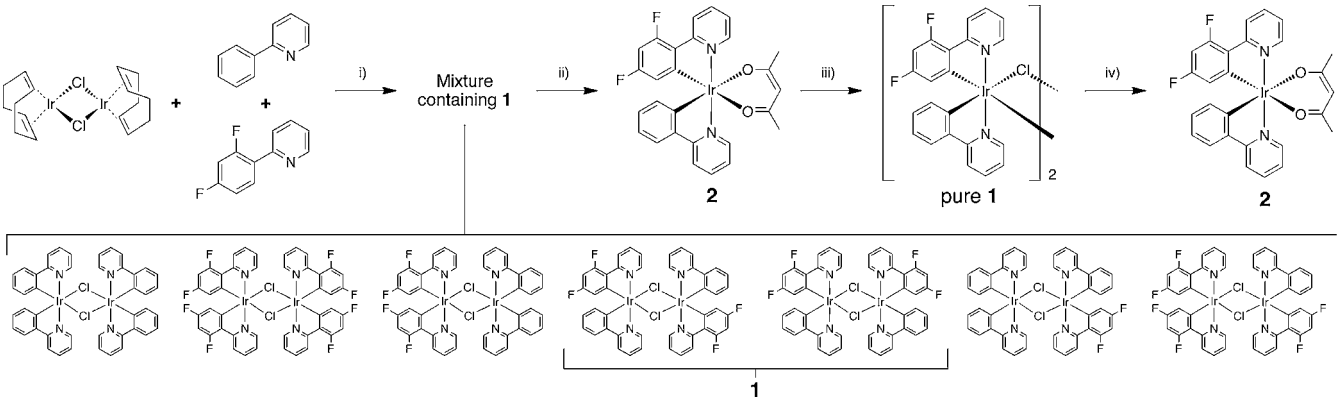

[a]Conditions: (i) 2-ethoxyethanol, 130 °C, 3 h, 87%; (ii) acacH, TBAOH, CH_2Cl_2, 40 °C overnight, 44%; (iii) HCl (2 M in Et_2O), CH_2Cl_2, RT, 15 min, 86%; (iv) acacNa, CH_2Cl_2/MeOH, 40 °C overnight, quantitative. The mixture of dimers is explicited at the bottom.

(Figure 4). This mixture is purified by column chromatography. The tris-heteroleptic complex **2** was obtained in 44% yield over

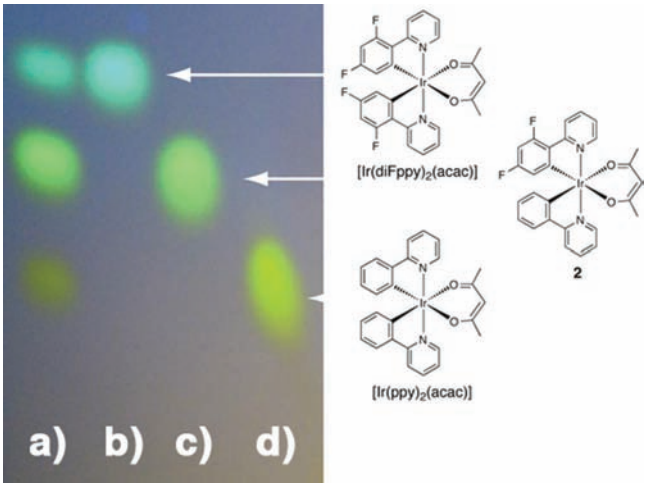

Figure 4. Thin layer chromatography (SiO_2, CH_2Cl_2) under UV illumination (365 nm): (a) crude of acac complexes obtained from the dimer mixture, (b) $Ir(diFppy)_2(acac)$, (c) **2**, (d) $Ir(ppy)_2(acac)$.

two steps, which is a significant improvement over the use of $IrCl_3$ starting materials. The ^{1}H NMR spectrum of **2** displays 14 aromatic signals while 6 and 8 aromatic signals are observed for the homoleptic complexes (Figure 5). The spectrum for the tris-heteroleptic complex is very close to the sum of the spectra for the two bis-heteroleptic complexes with one singlet for the acac at 5.23 ppm, that is an intermediate value for the same proton in $[Ir(ppy)_2(acac)]$ (5.21 ppm) and $[Ir(diFppy)_2(acac)]$ (5.24 ppm) (Figure 5). In addition, two singlets are observed for the methyl groups of the acac ligand, confirming the nonsymmetrical structure. The ^{19}F NMR spectrum shows two signals only slightly shifted compared to the signals for $[Ir(diFppy)_2(acac)]$. Finally, the high-resolution mass spectrum, elemental analysis, and X-ray crystal structure (see below) confirm the chemical structure of **2**.

Obtaining pure complex **2** is the key step that allows for the simple preparation of subsequent tris-heteroleptic complexes based on the [Ir(ppy)(diFppy)] fragment. Using our acid-induced degradation method, we could prepare pure heteroleptic chloro-bridged iridium dimer **1** in 86% isolated yield (38% from $[\{Ir(COD)(\mu\text{-}Cl)\}_2]$, compared to 50% maximum theoretical yield) by stirring **2** for 15 min at room temperature in the presence of HCl (Scheme 2). Figure 6a shows the ^{1}H NMR spectrum of the crude mixture of dimers containing **1** as obtained from the reaction of the ppy and diFppy ligands with $[\{Ir(COD)(\mu\text{-}Cl)\}_2]$ while Figure 6b shows the ^{1}H NMR of pure **1** as obtained after the reaction of **2** with HCl. Interestingly, the ^{1}H NMR of **1** is roughly the sum of the ^{1}H NMR spectra of $[\{Ir(ppy)_2(\mu\text{-}Cl)\}_2]$ (Figure 6c) and $[\{Ir(diFppy)_2(\mu\text{-}Cl)\}_2]$ (Figure 6d). On the other hand, the ^{1}H NMR spectrum of the initial crude reaction is not the simple addition of the ^{1}H NMR spectra of **1**, $[\{Ir(ppy)_2(\mu\text{-}Cl)\}_2]$, and $[\{Ir(diFppy)_2(\mu\text{-}Cl)\}_2]$, as it contains as well the dimers $[Ir_2(ppy)_{4-n}(diFppy)_n(\mu\text{-}Cl)_2]$ with n = 1 and 3.

To further support the chloro-bridged dimer formation, we added one drop of DMSO to the NMR tube. The addition of a coordinating solvent S to the chloro-bridged dimer cleanly breaks it and results generally in mononuclear complexes of the form $[Ir(C^N)_2(Cl)(S)]$.[43] In our case, addition of DMSO leads to two [Ir(ppy)(diFppy)(Cl)(DMSO)] isomeric complexes where the chloride is either trans to the phenyl of ppy or trans to the phenyl of diFppy. The ratio of the two isomers is roughly 3 to 2, pointing to a slight difference in reactivity of the two positions. A similar ratio is observed in the ^{19}F NMR spectrum. To verify that the acid-induced degradation has no impact on the geometry of the C^N ligands, we prepared **2** from pure **1** by refluxing **1** in dichloromethane in the presence of an excess of sodium acetylacetonate. The ^{1}H NMR spectrum of the crude of the reaction is virtually indistinguishable from the spectrum of purified **2** from reaction with the mixture of dimers (see Figures S15 and S17 of the Supporting Information). As we know the geometry of complex **2** from X-ray diffraction, this proves that the conditions used do not lead to trans−cis isomerization of the C^N ligands. Finally, with the pure heteroleptic dimer available, it is now possible to screen ancillary ligands for exploring the emission properties of such somplexes (Figure S3), as previously reported for homoleptic dimers.[44] As expected, in all cases tested, the emission of the tris-heteroleptic complex falls in between the emissions of the two homoleptic complexes. By following traditional synthetic procedures starting from chloro-bridged iridium(III) dimers, new tris-heteroleptic complexes are easily accessible from **1** without the need of tedious purification to

dx.doi.org/10.1021/ic202162q | Inorg. Chem. 2012, 51, 215−224

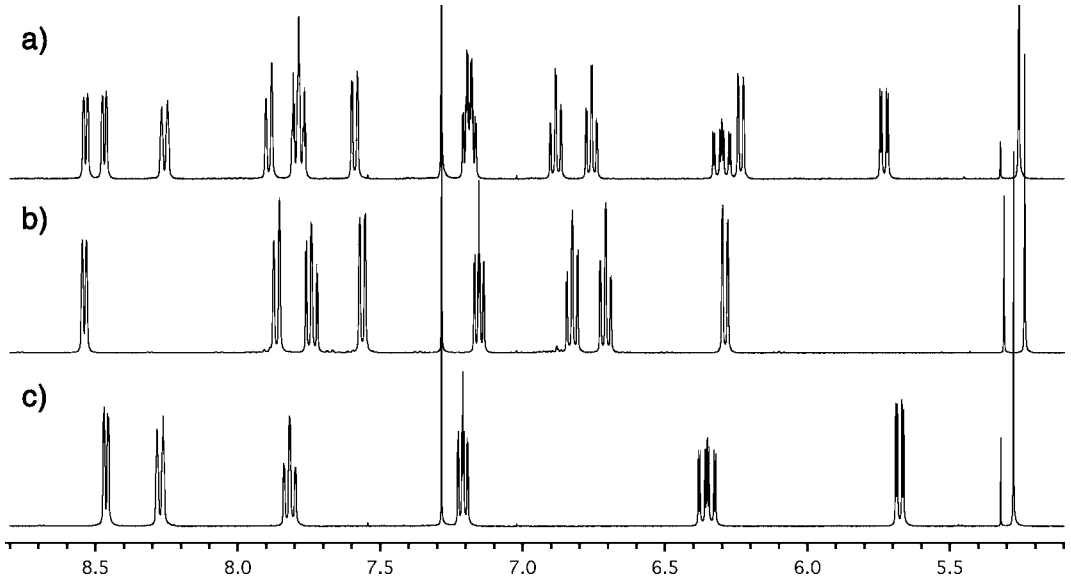

Figure 5. Aromatic part of ^{1}H NMR spectra ($CDCl_3$, 400 MHz) of (a) **2**, [Ir(ppy)(diFppy)(acac)]; (b) [Ir(ppy)$_2$(acac)]; (c) [Ir(diFppy)$_2$(acac)].

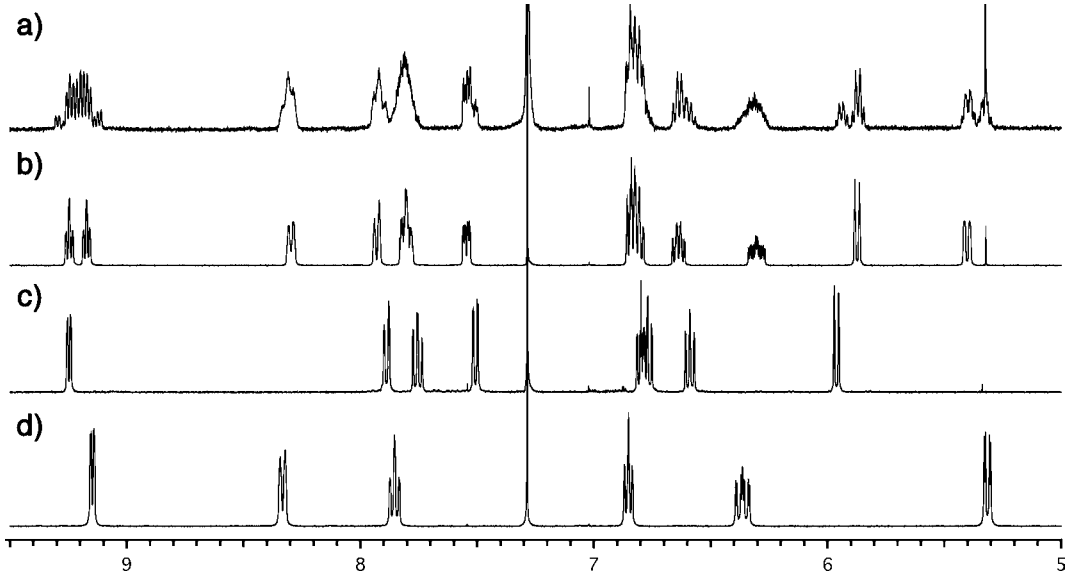

Figure 6. Aromatic part of ^{1}H NMR spectra ($CDCl_3$, 400 MHz) of (a) crude of the mixture of dimer containing **1**; (b) purified **1**; (c) [{Ir(ppy)$_2$(μ-Cl)}$_2$]; and (d) [{Ir(diFppy)$_2$(μ-Cl)}$_2$].

separate every time the tris-heteroleptic complex from the bis-homoleptic complexes.

X-ray Crystal Structure. Single crystals of **2** have been grown by slow diffusion of hexane into a dichloromethane solution of the complex. The structure is shown in Figure 7, and selected bond lengths and angles are given in Table 1 and compared with theoretical ground state geometries calculated for **2** both in gas phase and as a solvated molecule. Only minor changes are observed between the solvated and gas phase theoretical geometry, and both are very similar to the experimental values. The complex has the expected distorted octahedral geometry around the iridium center, with the two pyridines in trans positions relative to each other. Interestingly, the diFppy ligand appears more tightly bound to the iridium center, as both the Ir(1)−C(11) and Ir(1)−N(1) distances are slightly shorter than the corresponding distances for the ppy ligand.

Properties of Tris-heteroleptic Complexes. For all three acac complexes, the redox potentials measured in dimethylformamide are quasi-reversible (Figure S4 of the Supporting Information). Both the oxidation and reduction potentials of **2** are close to the average of values of the two bis-heteroleptic complexes (Table 2 and Figure S4). This suggests similar HOMO and LUMO localizations on both the phenyl ring and the iridium center and on the pyridine, respectively, as observed for most of the bis-heteroleptic cyclometalated iridium complexes. This view is further supported by DFT-calculations (see below). Similarly, the UV−visible absorption spectrum of **2** is close to the average of the two bis-heteroleptic complexes (Figure 8 and Table 2). When excited in the lowest ^{1}MLCT (metal-to-ligand charge-transfer) absorption band at room temperature, the complexes show emission at 484, 503, and 520 nm for [Ir(diFppy)$_2$(acac)], **2**, and [Ir(ppy)$_2$(acac)], respectively, with photoluminescence quantum yields of about

dx.doi.org/10.1021/ic202162q | *Inorg. Chem.* 2012, 51, 215−224

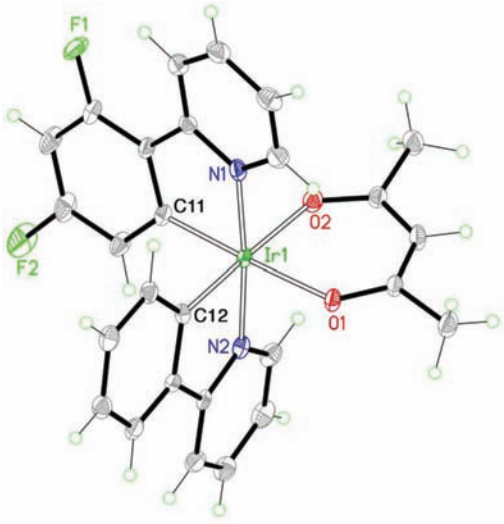

Figure 7. ORTEP representation of the X-ray crystal structure of **2**.

Table 1. Comparison between Experimental and Theoretical (DFT/M06) Ground State Geometries of Complex 2, Both Solvated and in the Gas Phase: Selected Bond Distances (Å) and Angles (deg)

	exptl	calcd gas phase	calc CH_2Cl_2
	Bond Distance		
Ir(1)−N(2)	2.050(4)	2.06	2.06
Ir(1)−N(1)	2.042(4)	2.05	2.06
Ir(1)−C(12)	1.997(5)	2.00	2.00
Ir(1)−C(11)	1.988(5)	2.00	2.00
Ir(1)−O(2)	2.162(4)	2.20	2.20
Ir(1)−O(1)	2.148(4)	2.19	2.19
	Bond Angle		
C(11)−Ir(1)−C(12)	89.70(19)	90.8	90.1
C(12)−Ir(1)−N(1)	95.43(19)	97.2	97.0
C(11)−Ir(1)−N(2)	95.64(19)	97.5	97.5
C(12)−Ir(1)−O(1)	90.65(17)	91.2	91.6
C(11)−Ir(1)−O(2)	91.41(17)	91.6	91.7
N(1)−Ir(1)−N(2)	174.60(17)	176.8	176.5

0.63, 0.69, and 0.47 for the three complexes and excited state lifetime on the microsecond time scale (Figure 8 and Table 2). When cooled to 77 K, the emission becomes strongly structured and the rigidochromic effect (the value ν_{max}(77 K) − ν_{max}(RT)) is in the 500−600 cm^{-1} range.[45] These two observations point to a ligand-centered (LC) excited state mixed with an MLCT state, as supported by DFT calculations (see below). Interestingly, the radiative constant (k_r) for **2** is about the average of the radiative constants for the homoleptic

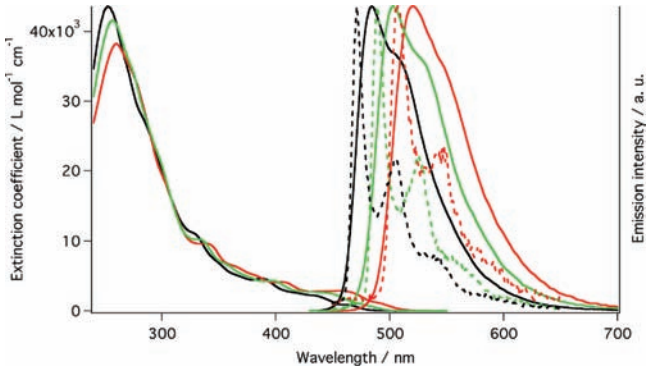

Figure 8. Absorption (left) and emission (right) spectra of $[Ir(ppy)_2(acac)]$ (red), $[Ir(diFppy)_2(acac)]$ (black), and **2** (green) in solution in dichloromethane. Dotted line: emission spectra at 77 K in 2-MeTHF.

complexes while the nonradiative constant (k_{nr}) is lower for **2** than for the homoleptic complexes.

This decrease of k_{nr} points to a localization of the excited state on only one of the C^N ligands, in contrast to homoleptic complexes, where the excited state might be delocalized over the two identical C^N ligands. Fewer vibrational modes will be available for nonradiative deactivation in the former case. This effect has been previously discussed[46] by comparing $[Ir(diFppy)_2(acac)]$ and $[Ir(diFppy)_2(pic)]$, where the localization of the excited state on a single diFppy ligand is due to the use of the nonsymmetric picolinate ancillary ligand. However, at that time it was not possible to rule out a specific effect of the picolinate on the accessibility of nonradiative metal-centered (MC) states or a difference in vibrational modes between acac and pic. These caveats do not apply in our case, as all complexes use the same acac ancillary ligand. Therefore, the decrease in nonradiative constant can be reasonably attributed to the localization of the excited-state on a single C^N ligand. It should be noted that the measured lifetimes of excited states are identical for $[Ir(ppy)_2(acac)]$ and for **2**: 1227 and 1224 ns, respectively. We believe that this result is fortuitous and is not representative of an excited state localized on the ppy ligand in complex **2**.

Information about the electronic structure of **2** was gained by DFT/LR-TDDFT calculations on the ground state (S_0) and the two first triplet excited states (T_{1a} and T_{1b}). As expected, compared to $[Ir(ppy)_2(acac)]$, the Kohn−Sham (KS) HOMO of **2** is at higher energy than the one of $[Ir(diFppy)_2(acac)]$, in agreement with the trend of computed ionization potentials. A difference of 0.19 eV in vertical ionization energy between $[Ir(diFppy)_2(acac)]$ and **2** was computed, which is in excellent

Table 2. Photo- and Electrochemical Properties of Homoleptic and Heteroleptic acac-Based Complexes

	λ_{abs} (nm), (ε (10^3L mol^{-1} cm^{-1})), RT[a]	λ_{em} (nm), RT[a]	τ (ns), RT[a]	Φ_{PL}[a]	λ_{em} (nm), 77 K[b]	k_r[c] (10^5 s^{-1})	k_{nr}[c] (10^5 s^{-1})	E_{ox} (V)[d]	E_{red} (V)[d]
$[Ir(ppy)_2(acac)]$	260 (38.26), 343 (9.46), 409 (4.06), 464 (2.75), 492 (1.08)	520	1227	0.47	507	3.83	4.32	0.41	−2.60
$[Ir(diFppy)_2(acac)]$	252 (43.59), 330 (10.93), 389 (4.64), 439 (2.02), 466 (0.80)	484	872	0.63	471	7.22	4.24	0.76	−2.44
2	256 (41.55), 335 (10.17), 399 (4.27), 449 (2.46), 478 (0.84)	503	1224	0.69	489	5.64	2.53	0.57	−2.52

[a]Degassed dichloromethane. [b]2-Methyltetrahydrofuran (2-MeTHF). [c]Assuming unitary intersystem crossing, $k_r = \Phi/\tau$ and $k_{nr} = (1 - \Phi)/\tau$. [d]Dimethylformamide/$TBAPF_6$ 0.1 M, vs Fc^+/Fc.

dx.doi.org/10.1021/ic202162q | Inorg. Chem. 2012, 51, 215−224

agreement with the experimental difference in oxidation potentials (Table 2).

The first two unoccupied orbitals of **2** are almost degenerate and are delocalized over the two ppy units, with an increased contribution from diFppy (LUMO) or ppy (LUMO+1) (Figure 9, upper-part). This suggests that the first electronic

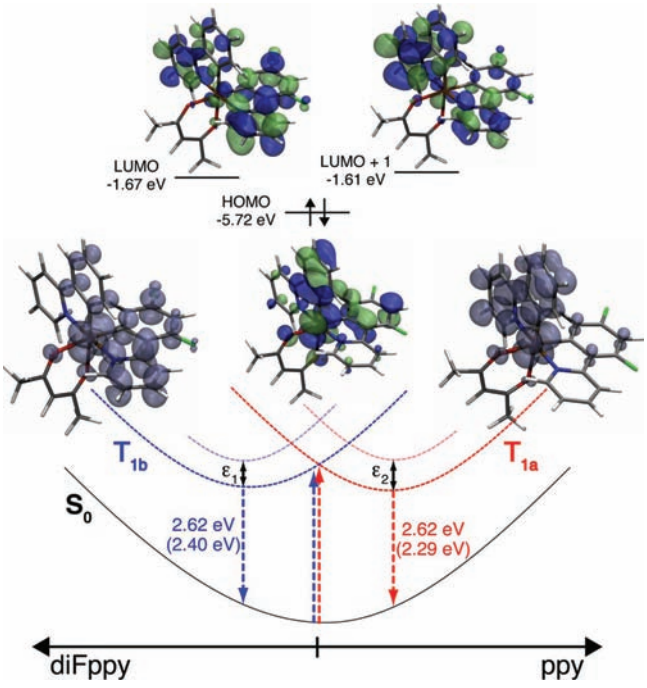

Figure 9. Schematic representation of the ground state (S_0, solid black line) and the first two triplet states (T_{1a} and T_{1b}, dashed red and blue lines) of compound **2** according to DFT calculations. Values between parentheses are emission energies according to ZORA/LR-TDDFT/M06. The abscissa represents the localization of the excited electron on the ppy or the diFppy ligand (ordinate is energy). The S_0 minimum geometry is located on the center of the abscissa, with the corresponding Kohn–Sham orbital representations and energies on the upper part (isovalue set to 0.03). On the right side: T_{1a} state with the related computed spin density distribution (isovalue of 0.003). On the left side: T_{1b} state with the related computed spin density distribution (isovalue of 0.003). ε_1 and ε_2 are equal to 0.28 and 0.48 eV, respectively (see text). Color code: Ir = ochre, C = gray, H = white, N = blue, O = red, F = green.

triplet states of **2** are likely to be formed by the transfer of one electron from a 5d(Ir) orbital to the ppy and diFppy ligands. LR-TDDFT/M06 calculations at the S_0 geometry support this fact, exhibiting two first triplet states at close energy (2.66 and 2.73 eV) formed by the population of LUMO and LUMO+1 orbitals. The T_{1a} (T_{1b}) excited state geometry has been obtained *via* the population of the KS LUMO+1 (or respectively LUMO) by one electron and performing U-DFT/M05-2X geometry optimizations. The two resulting triplet states can be described as MLCT/LC states. The excited electron is localized either on the ppy ligand (T_{1a}) or on the diFppy ligand (T_{1b}) and in both cases originates from a 5d(Ir) orbital with contributions from the C^N ligands (Figure 9). The difference in energy between the two triplet states and S_0 of **2** is 2.62 eV (exp: 2.47 eV, 2.54 eV at 77 K). A value of 2.78 eV (exp: 2.56 eV, 2.65 eV at 77 K) is found for [Ir(diFppy)$_2$(acac)], reproducing the experimental blue shift with respect to **2**. Spin–orbit calculations at the ZORA/LR-TDDFT/M06 level yield an emission energy of 2.40 eV (T_{1b}) and 2.29 eV (T_{1a}), and they point toward a faster emission from T_{1b} with a radiative lifetime of 5.3 μs compared to T_{1a} with 14.0 μs. The T_{1a} and T_{1b} excited states are computed to lie at almost equal DFT energies (T_{1a} being lower in energy by only 2 kJ/mol), but with different geometries due to the different localizations of the excited electrons. This results in the absence of close degeneracy of triplet states at either the T_{1a} or T_{1b} geometry, with the next higher lying triplet state being observed at 0.28 eV (from the T_{1b} geometry, ε_1 in Figure 9) or 0.48 eV (from the T_{1a} geometry, ε_2 in Figure 9) according to LR-TDDFT/M06. This lack of potential vibronic coupling may explain the rather thin emission profile of **2** in comparison to our previously reported broad emitter (acetylacetonato)bis(1-methyl-2-phenylimidazole)iridium(III).[47] We previously attributed the exceptionally broad emission of this emitter to almost degenerated LUMOs. We reasoned that, by having three different ligands instead of two, it would be possible to further improve the broadness of the emission, as done with the ancillary ligand.[44] To progress toward this goal, the new results about the tris-heteroleptic complexes stress the importance of the excited state degeneracy for designing future efficient single-center white emitters.

CONCLUSION

In this manuscript, we first report the efficient acid-induced cleavage of the N^O and O^O ancillary ligands in bis-cyclometalated iridium(III) complexes. We used chloridric acid, triflic acid, boron trifluoride, and PEDOT:PSS as acids. With chloride anions available, the cleavage of the ancillary ligand results in the formation of the chloro-bridged iridium(III) dimer. Our results link the observed sensitivity to acids of bis-heteroleptic iridium(III) complexes and the observed cleavage of the ancillary ligand in stressed electroluminescent devices. As protons can be present in the emissive layer, this study gives a possible chemical origin for the observed degradation of phosphorescent dopants in OLEDs.

Furthermore, we advantageously used this stability drawback to synthesize pure heteroleptic chloro-bridged iridium dimers. Such dimers can be further used for direct and simple preparation of new tris-heteroleptic iridium(III) complexes that are otherwise very challenging to synthesize. These tris-heteroleptic complexes have the potential to improve single center broad emitters. Importantly, theoretical calculations establish the importance of the excited state geometry to achieve this goal. Finally, our results tend to confirm the positive effect on the nonradiative constant of the dissymmetrization of the complex. It is attributed to the excited state being localized on a single chromophoric ligand, which decreases the number of vibrational modes available for nonradiative deactivation.

ASSOCIATED CONTENT

Supporting Information

Additional figures, ^{1}H NMR spectra, coordinates of computed complexes, and cif data. This material is available free of charge via the Internet at http://pubs.acs.org.

AUTHOR INFORMATION

Corresponding Author

*E-mail: etienne.baranoff@epfl.ch.

dx.doi.org/10.1021/ic202162q | *Inorg. Chem.* 2012, 51, 215–224

■ ACKNOWLEDGMENTS

We acknowledge financial support for this work by Solvay S.A., the European Union (CELLO, STRP 248043) and the Swiss National Science Foundation (NCCR-MUST interdisciplinary research program).

■ REFERENCES

(1) Baldo, M. A.; O'Brien, D. F.; You, Y.; Shoustikov, A.; Sibley, S.; Thompson, M. E.; Forrest, S. R. *Nature* **1998**, *395*, 151.
(2) Aziz, H.; Popovic, Z. D. *Chem. Mater.* **2004**, *16*, 4522.
(3) So, F.; Kondakov, D. *Adv. Mater.* **2010**, *22*, 3762.
(4) Giebink, N. C.; D'Andrade, B. W.; Weaver, M. S.; Brown, J. J.; Forrest, S. R. *J. Appl. Phys.* **2009**, *105*, 124514.
(5) Adachi, C.; Kwong, R. C.; Djurovich, P.; Adamovich, V.; Baldo, M. A.; Thompson, M. E.; Forrest, S. R. *Appl. Phys. Lett.* **2001**, *79*, 2082.
(6) Sivasubramaniam, V.; Brodkorb, F.; Hanning, S.; Loebl, H. P.; van Elsbergen, V.; Boerner, H.; Scherf, U.; Kreyenschmidt, M. *J. Fluorine Chem.* **2009**, *130*, 640.
(7) de Moraes, I. R.; Scholz, S.; Lüssem, B.; Leo, K. *Org. Electron.* **2011**, *12*, 341.
(8) Baranoff, E.; Suarez, S.; Bugnon, P.; Barolo, C.; Buscaino, R.; Scopelliti, R.; Zuppiroli, L.; Graetzel, M.; Nazeeruddin, M. K. *Inorg. Chem.* **2008**, *47*, 6575.
(9) Baranoff, E.; Bolink, H. J.; De Angelis, F.; Fantacci, S.; Di Censo, D.; Djellab, K.; Gratzel, M.; Nazeeruddin, M. K. *Dalton Trans.* **2010**, *39*, 8914.
(10) de Moraes, I. R.; Scholz, S.; Lüssem, B.; Leo, K. *Appl. Phys. Lett.* **2011**, *99*, 053302.
(11) Baranoff, E.; Barigelletti, F.; Bonnet, S.; Collin, J. P.; Flamigni, L.; Mobian, P.; Sauvage, J. P. *Struct. Bonding (Berlin)* **2007**, *123*, 41.
(12) Treboux, G.; Mizukami, J.; Yabe, M.; Nakamura, S. *Chem. Lett.* **2007**, *36*, 1344.
(13) Sajoto, T.; Djurovich, P. I.; Tamayo, A. B.; Oxgaard, J.; Goddard, W. A.; Thompson, M. E. *J. Am. Chem. Soc.* **2009**, *131*, 9813.
(14) Sivasubramaniam, V.; Brodkorb, F.; Hanning, S.; Buttler, O.; Loebl, H. P.; van Elsbergen, V.; Boerner, H.; Scherf, U.; Kreyenschmidt, M. *Solid State Sci.* **2009**, *11*, 1933.
(15) van Dijken, A.; Perro, A.; Meulenkamp, E. A.; Brunner, K. *Org. Electron.* **2003**, *4*, 131.
(16) Park, G. Y.; Kim, Y.; Ha, Y. *Mol. Cryst. Liq. Cryst.* **2007**, *462*, 179.
(17) Edkins, R. M.; Wriglesworth, A.; Fucke, K.; Bettington, S. L.; Beeby, A. *Dalton Trans.* **2011**, *40*, 9672.
(18) Felici, M.; Contreras-Carballada, P.; Smits, J. M. M.; Nolte, R. J. M.; Williams, R. M.; De Cola, L.; Feiters, M. C. *Molecules* **2010**, *15*, 2039.
(19) Duisenberg, A. J. M.; Kroon-Batenburg, L. M. J.; Schreurs, A. M. M. *J. Appl. Crystallogr.* **2003**, *36*, 220.
(20) Blessing, R. H. *Acta Crystallogr., Sect. A* **1995**, *51*, 33.
(21) Sheldrick, G. M. *Acta Crystallogr., Sect. A* **2008**, *64*, 112.
(22) Zhao, Y.; Truhlar, D. G. *Theor. Chem. Acc.* **2008**, *120*, 215.
(23) Hay, P. J.; Wadt, W. R. *J. Chem. Phys.* **1985**, *82*, 299.
(24) McLean, A. D.; Chandler, G. S. *J. Chem. Phys.* **1980**, *72*, 5639.
(25) Frisch, M. J.; Trucks, G. W.; Schlegel, H. B.; Scuseria, G. E.; Robb, M. A.; Cheeseman, J. R.; Scalmani, G.; Barone, V.; Mennucci, B.; Petersson, G. A.; Nakatsuji, H.; Caricato, M.; Li, X.; Hratchian, H. P.; Izmaylov, A. F.; Bloino, J.; Zheng, G.; Sonnenberg, J. L.; Hada, M.; Ehara, M.; Toyota, K.; Fukuda, R.; Hasegawa, J.; Ishida, M.; Nakajima, T.; Honda, Y.; Kitao, O.; Nakai, H.; Vreven, T.; Montgomery, J. J. A.; Peralta, J. E.; Ogliaro, F.; Bearpark, M.; Heyd, J. J.; Brothers, E.; Kudin, K. N.; Staroverov, V. N.; Kobayashi, R.; Normand, J.; Raghavachari, K.; Rendell, A.; Burant, J. C.; Iyengar, S. S.; Tomasi, J.; Cossi, M.; Rega, N.; Millam, J. M.; Klene, M.; Knox, J. E.; Cross, J. B.; Bakken, V.; Adamo, C.; Jaramillo, J.; Gomperts, R.; Stratmann, R. E.; Yazyev, O.; Austin, A. J.; Cammi, R.; Pomelli, C.; Ochterski, J. W.; Martin, R. L.; Morokuma, K.; Zakrzewski, V. G.; Voth, G. A.; Salvador, P.; Dannenberg, J. J.; Dapprich, S.; Daniels, A. D.; Farkas, Ö.; Foresman, J. B.; Ortiz, J. V.; Cioslowski, J.; Fox, D. J. *Gaussian 09*, Revision A.02; Gaussian, Inc.: Wallingford, CT, 2009.
(26) Tomasi, J.; Mennucci, B.; Cammi, R. *Chem. Rev.* **2005**, *105*, 2999.
(27) Scalmani, G.; Frisch, M. J.; Mennucci, B.; Tomasi, J.; Cammi, R.; Barone, V. *J. Chem. Phys.* **2006**, *124*, 094107.
(28) Swiderek, K.; Paneth, P. *J. Phys. Org. Chem.* **2009**, *22*, 845.
(29) Zhao, Y.; Schultz, N. E.; Truhlar, D. G. *J. Chem. Theory Comput.* **2006**, *2*, 364.
(30) Fonseca Guerra, C.; Snijders, J. G.; te Velde, G.; Baerends, E. J. *Theor. Chem. Acc.* **1998**, *99*, 391.
(31) te Velde, G.; Bickelhaupt, F. M.; van Gisbergen, S. J. A.; Fonseca Guerra, C.; Baerends, E. J.; Snijders, J. G.; Ziegler, T. *J. Comput. Chem.* **2001**, *22*, 931.
(32) Wang, F.; Ziegler, T.; van Lenthe, E.; van Gisbergen, S. J. A.; Baerends, E. J. *J. Chem. Phys.* **2005**, *122*, 204103.
(33) Klamt, A.; Schüürmann, G. *J. Chem. Soc., Perkin Trans. 2* **1993**, 799.
(34) Pye, C. C.; Ziegler, T. *Theor. Chem. Acc.* **1999**, *101*, 396.
(35) Baranoff, E.; Suarez, S.; Bugnon, P.; Bolink, H. J.; Klein, C.; Scopelliti, R.; Zuppiroli, L.; Grätzel, M.; Nazeeruddin, M. K. *ChemSusChem* **2009**, *2*, 305.
(36) Dedeian, K.; Djurovich, P. I.; Garces, F. O.; Carlson, G.; Watts, R. J. *Inorg. Chem.* **1991**, *30*, 1685.
(37) Deaton, J. C.; Young, R. H.; Lenhard, J. R.; Rajeswaran, M.; Huo, S. Q. *Inorg. Chem.* **2010**, *49*, 9151.
(38) Gill, R. E.; van de Weijer, P.; Leiedenbaum, C. T. H.; Schoo, H. F. M.; Berntsen, A.; Vleggaar, J. J. M.; Visser, R. J. *Opt. Mater.* **1999**, *12*, 183.
(39) Lamansky, S.; Djurovich, P.; Murphy, D.; Abdel-Razzaq, F.; Kwong, R.; Tsyba, I.; Bortz, M.; Mui, B.; Bau, R.; Thompson, M. E. *Inorg. Chem.* **2001**, *40*, 1704.
(40) Tsurugi, H.; Fujita, S.; Choi, G.; Yarnagata, T.; Ito, S.; Miyasaka, H.; Mashima, K. *Organometallics* **2010**, *29*, 4120.
(41) Sasabe, H.; Takamatsu, J.-I.; Motoyama, T.; Watanabe, S.; Wagenblast, G.; Langer, N.; Molt, O.; Fuchs, E.; Lennartz, C.; Kido, J. *Adv. Mater.* **2010**, *22*, 5003.
(42) Böttcher, H. C.; Graf, M.; Sunkel, K.; Mayer, P.; Kruger, H. *Inorg. Chim. Acta* **2011**, *365*, 103.
(43) Sprouse, S.; King, K. A.; Spellane, P. J.; Watts, R. J. *J. Am. Chem. Soc.* **1984**, *106*, 6647.
(44) Baranoff, E.; Jung, I.; Scopelliti, R.; Solari, E.; Grätzel, M.; Nazeeruddin, M. K. *Dalton Trans.* **2011**, *40*, 6860.
(45) Tsuboyama, A.; Iwawaki, H.; Furugori, M.; Mukaide, T.; Kamatani, J.; Igawa, S.; Moriyama, T.; Miura, S.; Takiguchi, T.; Okada, S.; Hoshino, M.; Ueno, K. *J. Am. Chem. Soc.* **2003**, *125*, 12971.
(46) Rausch, A. F.; Thompson, M. E.; Yersin, H. *J. Phys. Chem. A* **2009**, *113*, 5927.
(47) Bolink, H. J.; De Angelis, F.; Baranoff, E.; Klein, C.; Fantacci, S.; Coronado, E.; Sessolo, M.; Kalyanasundaram, K.; Grätzel, M.; Nazeeruddin, M. K. *Chem. Commun.* **2009**, 4672.